

Disturbance Rejection in Repetitive-Control Systems Based on Equivalent-Input-Disturbance Approach

Min Wu, Baogang Xu, Weihua Cao, and Jinhua She

Abstract—Since a repetitive control system can track a periodic reference input and reject a periodic disturbance perfectly, it has been widely applied in control engineering practice. However, the disturbance-rejection performance is not satisfactory for a non-periodic disturbance or for a periodic disturbance with a period different from that of the repetitive controller. To solve this problem, this paper presents a new configuration of a repetitive control system that incorporates an equivalent-input-disturbance estimator. A sufficient stability criterion is derived based on the separation and small gain theorems. A design algorithm is developed for the system based on the stability criterion. Simulation results of a disk drive servo system are used to verify the effectiveness of the method.

I. INTRODUCTION

In control engineering practice, many systems, for example, a disk drive system, an electronic power system, and a motor system, are required to track periodic reference inputs and/or reject periodic disturbances. To meet this need, Inoue *et al.* proposed a control strategy called repetitive control (RC) [1] based on an internal model principle [2]. It enables perfect tracking or rejection of periodic signals. Over the past a couple of decades, a great number of studies have been made on the theory and applications [3]–[8].

One problem with a repetitive control system (RCS) is that, if a disturbance has frequency components other than those at the fundamental and harmonic frequencies of the repetitive controller, then the RCS cannot reject this disturbance. Some strategies have been proposed to solve this problem. For example, a disturbance observer (DOB) has been introduced in an RCS [9]. But the design of a low-pass filter, $Q(s)$, in the DOB is complicated because it has to guarantee both the causality of the DOB and the stability of the system. Kim *et al.* proposed a two-parameter robust RCS to reject both periodic and non-periodic disturbances using the discrete-time μ -synthesis and an H_∞ control method [10]. However, the order of a designed controller is very high and is hard to implement in practice. A high order repetitive controller was also presented to improve the performance of disturbance rejection at intermediate frequencies [5], [11]. But it might be difficult to obtain a satisfactory disturbance-

attenuation level due to the trade-off between the robustness and the disturbance-rejection performance for the system.

Recently, an active disturbance-rejection method called an equivalent-input-disturbance (EID) approach has been presented [12], [13]. Since the controller in the system has two degrees of freedom; it not only can reject various kinds of disturbances effectively, but also is easy to implement.

This study applies the EID approach to an RCS to improve the tracking and disturbance-rejection performance. In this paper, we first present the structure of an EID-based RCS. Then, based on the separation and small gain theorems, we derive a stability criterion by dividing the system into two subsystems: repetitive control and EID estimation. This allows the independent design of the repetitive controller and the EID estimator. Finally, we demonstrate the validity of the method through simulations.

Throughout this paper, I denotes a unit matrix of suitable dimensions; N^T means the transpose of matrix N ; \mathbb{R}^n is the n -dimensional Euclidean space; $\mathbb{R}_+^{p \times m}$ is a set of the proper stable rational $p \times m$ matrices; and $\|G\|_\infty := \sup_{0 \leq \omega < \infty} \sigma_{\max}[G(j\omega)]$ denotes the infinity norm of $G(s)$ ($G(s) \in \mathbb{R}_+^{p \times m}$) and $\sigma_{\max}[G]$ is the maximum singular value of the matrix $G(s)$.

II. EID APPROACH

Before introducing the EID approach into an RCS, we give the definition of an EID and preliminaries in this section.

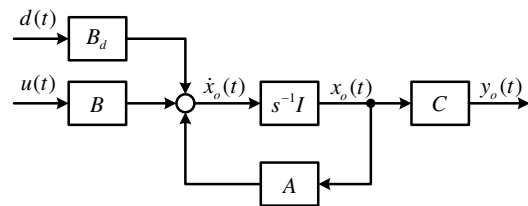


Fig. 1. Plant with disturbance.

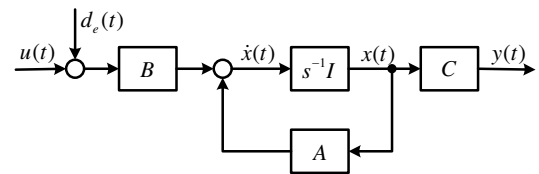


Fig. 2. Plant with EID.

This work was supported by the National Natural Science Foundation of China under Grants 60974045 and 60674016, the National Science Fund for Distinguished Youth Scholars of China under Grant 60425310, and the Graduate Education Innovation Project of Central South University under Grant 2010ssxt197.

M. Wu, B. Xu, and W. Cao are with the School of Information Science and Engineering, University of Central South University, Changsha, 410083, China. E-mail: min@csu.edu.cn

J. She is with School of Computer Science, Tokyo University of Technology, Hachioji, Tokyo, 192-0982, Japan.

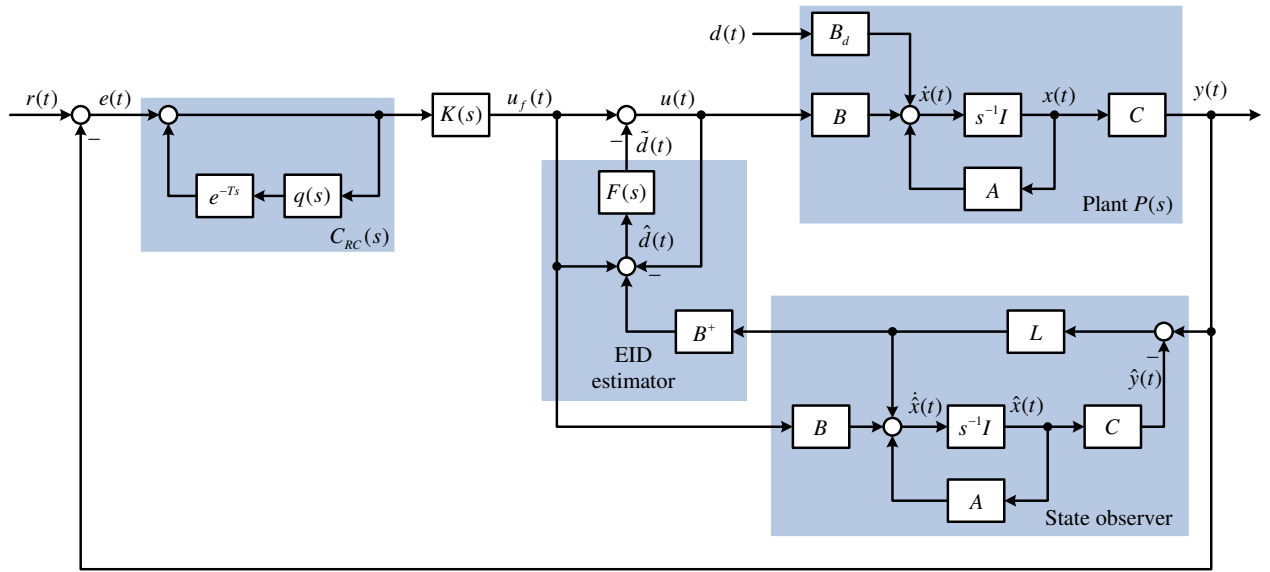


Fig. 3. Structure of EID-based RCS.

First, we recall the concept of an EID [12]. Fig. 1 shows a linear time-invariant plant affected by a disturbance, $d(t)$,

$$\begin{cases} \dot{x}_o(t) = Ax_o(t) + Bu(t) + B_d d(t) \\ y_o(t) = Cx_o(t). \end{cases} \quad (1)$$

And Fig. 2 shows the plant with a disturbance, $d_e(t)$,

$$\begin{cases} \dot{x}(t) = Ax(t) + B[u(t) + d_e(t)] \\ y(t) = Cx(t). \end{cases} \quad (2)$$

In (1) and (2), $A \in \mathbb{R}^{n \times n}$; $B \in \mathbb{R}^{n \times n_u}$; $B_d \in \mathbb{R}^{n \times n_d}$; $C \in \mathbb{R}^{n_y \times n}$; $x_o(t), x(t) \in \mathbb{R}^n$; $y_o(t), y(t) \in \mathbb{R}^{n_y}$; $d(t) \in \mathbb{R}^{n_d}$; and $u(t), d_e(t) \in \mathbb{R}^{n_u}$.

(A, B, C) satisfies the following assumptions.

Assumption 1: (A, B, C) is controllable and observable.

Assumption 2: (A, B, C) has no zeros on the imaginary axis.

The above assumptions are standard for the design of a servo system [14].

Definition 1 ([12]): In Figs. 1 and 2, let the control input $u(t) = 0$ and $x(0) = x_o(0) = 0$. If the output of Plant (1) for disturbance $d(t)$ and the output of Plant (2) for disturbance $d_e(t)$ satisfy $y(t) \equiv y_o(t), \forall t \geq 0$, then $d_e(t)$ is an EID of $d(t)$.

Define

$$\Phi = \{p_i(t) \sin(\omega_i t + \varphi_i)\}, \quad i = 0, 1, \dots, n, \quad n < \infty$$

where $\omega_i (\geq 0)$ and φ_i are constants, and $p_i(t)$ denotes any polynomial in time t ($i = 0, 1, \dots, n$); we have the following lemma regarding the existence of an EID.

Lemma 1 ([12]): Under Assumptions 1 and 2, if $y_o(t) \in \Phi$, then there exists an EID, $d_e(t) (\in \Phi)$, on the control input channel of Plant (1).

The EID approach is to produce an EID, $d_e(t)$, of the real disturbance, $d(t)$, and then impose it on the control input channel of the plant to cancel the effect of $d(t)$ on $y(t)$. So, the key point of the EID approach is to design an EID estimator that estimates the EID precisely.

III. DESIGN OF EID-BASED RCS

In this section, we first show the structure of the EID-based RCS. Next, we explain how to estimate an EID. Then, we carry out stability analysis and the design of the system. In this paper, we only consider the single-input single-output (SISO) system, that is, $n_u = 1$ and $n_y = 1$.

Fig. 3 shows the structure of the EID-based RCS. The system contains the plant, $P(s)$, a modified repetitive controller (MRC), $C_{RC}(s)$, a feedback compensator, $K(s)$, a state observer, and an EID estimator. In the figure,

$$B^+ := \frac{B^T}{B^T B}. \quad (3)$$

In the MRC, $q(s)$ is a low-pass filter that relaxes the stability condition, and T is the delay time of the MRC. The MRC is used to track a periodic reference or reject a periodic disturbance with the fundamental frequency being $1/T$.

L is the state observer gain. $F(s)$ is a low-pass filter. The disturbance-rejection performance of the RCS is improved by incorporating the EID estimate into the original repetitive control law.

A. Estimation of the EID

In Fig. 3, the state observer is

$$\dot{\hat{x}}(t) = A\hat{x}(t) + Bu_f(t) + L[y(t) - C\hat{x}(t)] \quad (4)$$

where $\hat{x}(t) \in \mathbb{R}^n$ is the state of the observer.

Defining the error of state estimation to be

$$\Delta x(t) = \hat{x}(t) - x(t) \quad (5)$$

and substituting (5) into (2) yield

$$\dot{\hat{x}}(t) = A\hat{x}(t) + Bu(t) + \{Bd_e(t) + [\Delta\dot{x}(t) - A\Delta x(t)]\}. \quad (6)$$

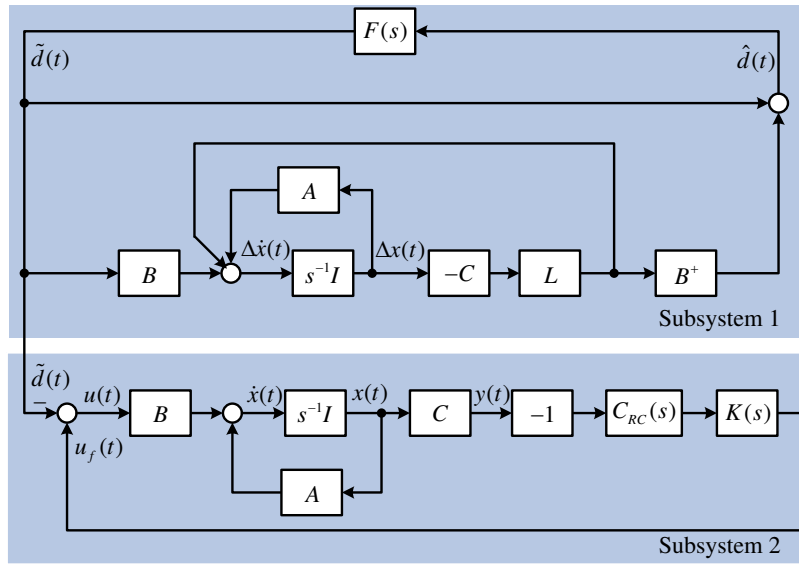


Fig. 4. Equivalent system of Fig. 3.

If we introduce a variable $\Delta d(t)$ that satisfies

$$B\Delta d(t) = \Delta \dot{x}(t) - A\Delta x(t) \quad (7)$$

substitute (7) into (6), and define an estimation of the EID, $d_e(t)$, as

$$\hat{d}(t) = d_e(t) + \Delta d(t) \quad (8)$$

then, we can write the plant as

$$\dot{\hat{x}}(t) = A\hat{x}(t) + B[u(t) + \hat{d}(t)]. \quad (9)$$

According to (4) and (9), we have

$$B[\hat{d}(t) + u(t) - u_f(t)] = LC[x(t) - \hat{x}(t)]. \quad (10)$$

Solving (10) for $\hat{d}(t)$ yields

$$\hat{d}(t) = B^+LC[x(t) - \hat{x}(t)] + u_f(t) - u(t). \quad (11)$$

The low-pass filter, $F(s)$, is used to select the bandwidth of the estimation of $d_e(t)$. As a result, the filtered estimation of $d_e(t)$, which is denoted by $\tilde{d}(t)$, is

$$\tilde{D}(s) = F(s)\hat{D}(s) \quad (12)$$

where $\tilde{D}(s)$ and $\hat{D}(s)$ are the Laplace transforms of $\tilde{d}(t)$ and $\hat{d}(t)$, respectively.

The control input is modified to be

$$u(t) = u_f(t) - \tilde{d}(t) \quad (13)$$

so as to use $\tilde{d}(t)$ to suppress the effect of $d(t)$. Clearly, the disturbance-rejection performance depends on the estimation precision of the EID estimator.

B. Stability Criterion

Letting

$$G_1(s) = 1 - B^+LC[sI - (A - LC)]^{-1}B \quad (14)$$

$$P(s) = C(sI - A)^{-1}B \quad (15)$$

$$G(s) = K(s)P(s) \quad (16)$$

using the separation theorem and the small gain theorem, we derived the following stability criterion for the EID-based RCS.

Theorem 1: The EID-based RCS (Fig. 3) is stable if the following conditions are satisfied

- (a) Both $G_1(s)$ and $F(s)$ are stable;
- (b) $\|G_1F\|_\infty < 1$;
- (c) $[1 + G(s)]^{-1}G(s) \in \mathbb{R}_-$, and no unstable pole-zero cancellation occurs between $K(s)$ and $P(s)$; and
- (d) $\|q[1 + G]^{-1}\|_\infty < 1$.

Proof: Since a reference input and a disturbance do not affect the stability of the control system, for simplicity, we let

$$r(t) = 0, \quad d(t) = 0.$$

Then, the plant becomes

$$\dot{x}(t) = Ax(t) + Bu(t) \quad (17)$$

where $u(t)$ is given by (13).

Based on (4), (5), (13), and (17), we have

$$\Delta \dot{x}(t) = (A - LC)\Delta x(t) + B\tilde{d}(t). \quad (18)$$

And from (5) and (13), it is clear that (11) can be written as

$$\hat{d}(t) = -B^+LC\Delta x(t) + \tilde{d}(t). \quad (19)$$

We redraw Fig. 3 as Fig. 4. It can be seen that the EID-based RCS has been decomposed into two subsystems in series:

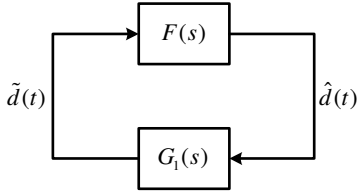


Fig. 5. Block diagram of Subsystem 1.

Subsystem 1 (above) and Subsystem 2 (below). Since there does not exist a loop between them, the stability of the whole system is equivalent to that both Subsystems 1 and 2 are stable. So, as long as stability is the only consideration, these two subsystems can be analyzed and designed separately. Since Subsystems 1 and 2 contain parameters only related to the EID estimator and to the MRC, respectively, we can design them independently. This also shows that the EID estimator can be plugged into the RCS directly if the stability of Subsystem 1 is guaranteed.

For Subsystem 1, according to (18) and (19), the transfer function from $\tilde{d}(t)$ to $\hat{d}(t)$ is (14). Redrawing Subsystem 1 in Fig. 4 yielded Fig. 5. It is clear from the small gain theorem [15] that Subsystem 1 is stable if Conditions (a) and (b) hold.

Subsystem 2 is a conventional RCS. According to [3], it is stable if Conditions (c) and (d) are satisfied.

This gives Conditions (a)-(d). ■

Remark 1: In Theorem 1, $G_1(s)$ is stable means that $A - LC$ is stable. So, Condition (a) ensures the convergence of the state observer (4), and Condition (b) guarantees the stability of the system after inserting the EID estimator.

C. System Design

Now, we show the design procedure for the EID-based RCS.

First, we design $F(s)$ and L , which are related to the EID estimation in Fig. 3.

For the design of the low-pass filter, $F(s)$, according to the relationship between the characteristic of $F(s)$ and the performance of the EID estimator, which was studied in [12], a first-order low-pass filter

$$F(s) = \frac{K_f}{s + \omega_f} \quad (20)$$

was selected, where $K_f (> 0)$ is a constant and ω_f is the cut-off angular frequency of the filter. It should satisfy Condition (a) in Theorem 1. And ω_f should be selected larger than the highest angular frequency of the disturbance to be rejected.

We employed the pole placement method, which is commonly used to design the gain of a state observer or state feedback, to find an L . Since the poles to be assigned determine the performance of the state observer and thus that of the EID estimator, they should be selected carefully. In the selection of L , Condition (b) in Theorem 1, poles of the plant, and characteristics of the disturbance should be taken into account.

Now, we consider the design of the low-pass filter, $q(s)$, in the MRC and the feedback compensator, $K(s)$. $q(s)$ was chosen based on the required tracking performance for the reference. $K(s)$ is used to ensure that the basic feedback system, which contains only $K(s)$ and $P(s)$, satisfy Conditions (c) and (d) in Theorem 1, and has sufficient gain and phase margins. These guarantee that the EID-based RCS can easily satisfy the desired requirements, such as control bandwidth, loop gain, etc. $q(s)$ and $K(s)$ can easily be designed using an existing method, for example, [3], [16], [17].

IV. NUMERICAL EXAMPLE

The effectiveness of the EID-based RCS is demonstrated through the simulations of the tracking-following servo system of an optical disk drive.

A. Description of Plant

$r(t)$ and $y(t)$ are the desired and real positions of the laser beam spot, $e(t)$ is the tracking error, and $d(t)$ is a disturbance.

The model of the plant, $P(s)$, is [4]

$$P(s) = \frac{76.35}{s^2 + 62s + 153675.5} \text{ m/V}. \quad (21)$$

Its state space representation is

$$\begin{cases} \dot{x}(t) = Ax(t) + B[u(t) + d(t)] \\ y(t) = Cx(t) \end{cases} \quad (22)$$

where

$$A = \begin{bmatrix} 0 & 1 \\ -153675.5 & -62 \end{bmatrix}, B = \begin{bmatrix} 0 \\ 76.35 \end{bmatrix}, C = [1 \quad 0].$$

The plant is subjected to two kinds of disturbances: a repeatable runout disturbance (RRD) and a non-repeatable runout disturbance (NRRD). While the RRD is synchronous with the disk rotational speed, the NRRD is asynchronous with the disk rotational speed. So, in this study, the disturbance, $d(t)$, which is a combination of

$$d_1(t) = 100000[0.7 \sin(80\pi t) + 0.2 \sin(160\pi t)]$$

$$d_2(t) = \begin{cases} 0, & 0 \leq t < 0.3 \\ 40000[\tanh(t-2) - \tanh(t-0.3)], & 0.3 \leq t \end{cases}$$

and

$$d_3(t) = 4000[2 \sin(177\pi t) + 2 \sin(277\pi t) + \sin(377\pi t)]$$

was added to the system. Clearly, $d_1(t)$ is an RRD with the period being 0.025 s. $d_2(t)$ and $d_3(t)$ are NRRDs. More specifically, $d_2(t)$ is a non-periodic disturbance, and $d_3(t)$ is a periodic disturbance with a period different from that of $d_1(t)$.

A simple check shows that Plant (22) satisfies Assumptions 1 and 2. So, based on Lemma 1, we know that the EID approach is applicable.

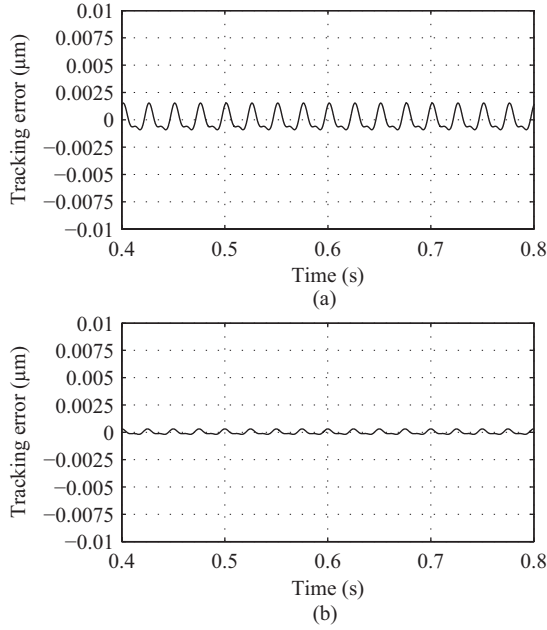


Fig. 6. Steady-state tracking error for $d(t) = d_1(t)$: (a) conventional RCS; (b) EID-based RCS.

B. Design of Controllers

The control objective is to ensure that the tracking error is within the range of $[-0.01, 0.01] \mu\text{m}$.

An EID-based RCS (Fig. 3) was designed to improve the disturbance-rejection performance and to achieve the control objective.

The bandwidth of the basic servo control system should be as high as about 3 kHz and the loop gain should be larger than 70 dB in the low-frequency band. A satisfactory compensator $K(s)$ is [4]

$$K(s) = \frac{3.87 \times 5.4 \times 10^6 (s + 1364)(s + 9425)}{(s + 942)(s + 87965)}. \quad (23)$$

Since the disk is required to rotate at a constant angular speed of 2400 rpm, the period of the RRD is 0.025 s. The parameters of the MRC in Fig. 3 were selected to be

$$T = 0.025 \text{ s}, \quad q(s) = \frac{5000\pi}{s + 5000\pi}. \quad (24)$$

Clearly, the period of the RRD, $d_1(t)$, is exactly the same as that of the MRC. But the period of $d_3(t)$ is different from that of the RC. The poles of Plant (21) are $p = -30 \pm j390.8$. We chose $F(s)$ to be

$$F(s) = \frac{0.8366 \times 5000\pi}{s + 5000\pi}$$

and chose the poles of the state observer to be

$$p = -830 \pm j800.$$

It yielded

$$L = [7047.46 \quad 5358.06]^T.$$

Simple calculation shows that $G_1(s)$ and $F(s)$ are stable, $\|G_1 F\|_\infty = 0.9997 < 1$, $[1 + G(s)]^{-1}G(s)$ is stable, there does

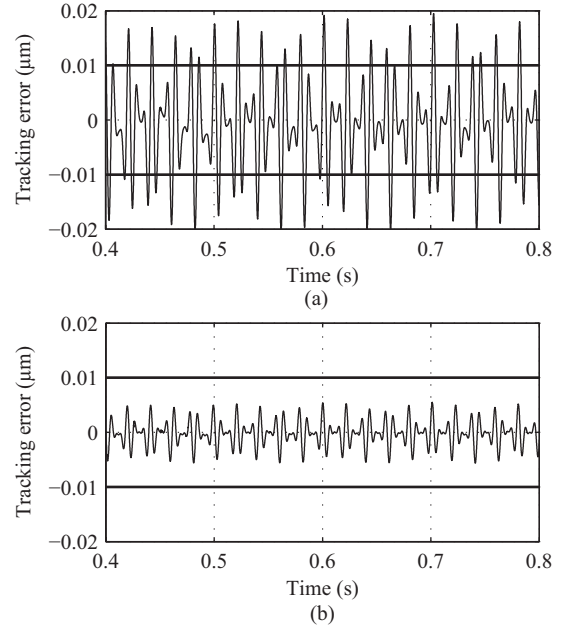


Fig. 7. Steady-state tracking error for $d(t) = d_1(t) + d_2(t) + d_3(t)$: (a) conventional RCS; (b) EID-based RCS.

not have pole-zero cancellation between $K(s)$ and $P(s)$, and $\|q[1 + G]^{-1}\|_\infty = 0.71263 < 1$. So, the conditions in Theorem 1 hold. And the EID-based RCS is stable.

C. Simulations

The tracking performance of the conventional RCS (without EID estimation) and the EID-based RCS for a disturbance contained only the RRD, $d_1(t)$, were first tested. The steady-state tracking errors were both in the range of $\pm 0.01 \mu\text{m}$ (Fig. 6). It is clear that we could achieve the control objective using the conventional RCS. And we further reduced the tracking error from the range of $\pm 0.0015 \mu\text{m}$ to $\pm 0.0003 \mu\text{m}$ by inserting the EID estimator.

Then, the tracking performance of the conventional RCS and EID-based RCS for a disturbance containing both the RRD and NRRD, $d(t) = d_1(t) + d_2(t) + d_3(t)$, were tested (Figs. 7 and 8).

Comparing Figs. 6 (a) with 7 (a), we can see that the NR-RDs, $d_2(t)$ and $d_3(t)$, deteriorated the tracking performance largely. As a result, the steady-state tracking error of the conventional RCS increased from the range of $\pm 0.0015 \mu\text{m}$ to $\pm 0.02 \mu\text{m}$. This made the conventional RCS did not achieve the control objective anymore. On the other hand, as shown in Fig. 7 (b), the disturbance-rejection performance was improved by introducing the EID estimator into the conventional RCS, and the steady-state tracking error was reduced from the range of $\pm 0.02 \mu\text{m}$ to $\pm 0.0056 \mu\text{m}$. So, the EID-based RCS made it possible to achieve the control objective.

The transient tracking error is shown in Fig. 8. In the figure, d_1 and $d_3(t)$ were imposed on the system from $t = 0$, and $d_2(t)$ was imposed from $t = 0.3$ s. It is clear from (a) and (b) in Fig. 8 that, introducing the EID estimator into the

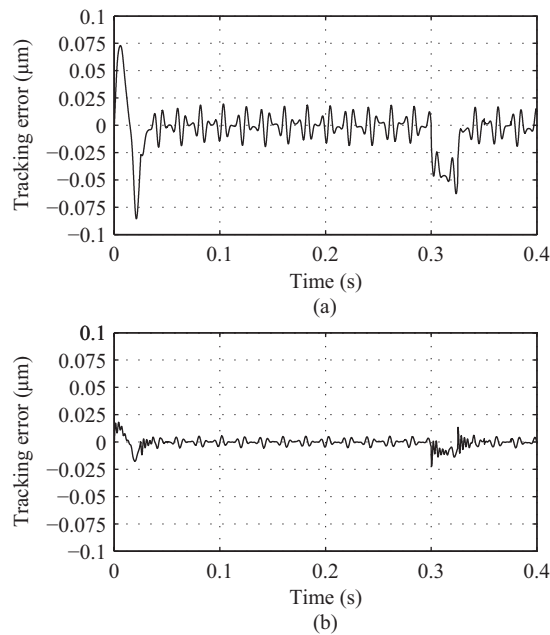


Fig. 8. Transient tracking error for $d(t) = d_1(t) + d_2(t) + d_3(t)$: (a) conventional RCS; (b) EID-based RCS.

conventional RCS decreased the maximum transient tracking error for d_1 and $d_3(t)$ from 0.086 to 0.018, and the maximum transient tracking error for $d_2(t)$ from 0.062 to 0.022. So, the transient response was also improved by inserting the EID estimator.

These simulation results show that inserting the EID estimator in the conventional RCS improved both the transient and steady-state disturbance-rejection performance, and thus the tracking performance.

V. CONCLUSION

This study developed a new repetitive-control system based on the EID approach. The introduction of the EID estimator improved the disturbance-rejection performance, in particular for a non-periodic disturbance and a periodic disturbance with a period different from that of the RC. Since those disturbances are precisely estimated by the EID estimator, combining the disturbance estimate with the feedback control law rejected the disturbance effectively and improved the tracking performance.

One distinguished advantage of this method is that the analysis and design of the repetitive controller and the EID estimator can be performed separately. This simplifies the design of the system. This fact also indicates that a

stable EID estimator can be directly plugged into an RCS. Simulation results of the tracking-following servo system of an optical disk drive demonstrated the effectiveness of the method.

REFERENCES

- [1] T. Inoue, M. Nakano, and S. Iwai, "High Accuracy Control of a Proton Synchrotron Magnet Power Supply," in *Proceedings of the 8th World Congress of IFAC*, Kyoto, Japan, 1981, Part 3, pp 3137-3142.
- [2] B. A. Francis and W. M. Wonham, "The Internal Model Principle for Linear Multivariable Regulators," *Applied Mathematics & Optimization*, 1975, vol. 2, pp 170-194.
- [3] S. Hara, Y. Yamamoto, T. Omata, and M. Nakano, "Repetitive Control System: a New Type Servo System for Periodic Exogenous Signals," *IEEE Transactions on Automatic Control*, 1988, vol. 33, pp 659-666.
- [4] T. Y. Doh, J. R. Ryoo, and M. J. Chung, "Design of a Repetitive Controller: an Application to the Track-Following Servo System of Optical Disk Drives," *IEE Proc. Control Theory & Appl.*, 2006, vol. 153, pp 323-330.
- [5] M. Steinbuch, S. Weiland, and T. Singh, "Design of Noise and Period-Time Robust High-Order Repetitive Control, with Application to Optical Storage," *Automatica*, 2007, vol. 43, pp 2086-2095.
- [6] N. O. Pérez-Arancibia, T. C. Tsao, and J. S. Gibson, "A New Method for Synthesizing Multiple-Period Adaptive-Repetitive Controllers and its Application to the Control of Hard Disk Drives," *Automatica*, 2010, vol. 46, pp 1186-1195.
- [7] S. L. Chen and T. H. Hsieh, "Repetitive Control Design and Implementation for Linear Motor Machine Tool," *International Journal of Machine Tools & Manufacture*, 2007, vol. 47, 2007, pp 1807-1816.
- [8] K. Zhou, D. Wang, B. Zhang, and Y. Wang, "Plug-in Dual-Mode-Structure Repetitive Controller for CVCF PWM Inverters," *IEEE Transactions on Industrial Electronics*, 2009, vol. 56, pp 784-791.
- [9] C. Smith and M. Tomizuka, "Shock Rejection for Repetitive Control Using a Disturbance Observer," in *Proceedings of the 35th Conference on Decision and Control*, Kobe, Japan, 1996, pp 2503-2504.
- [10] B. S. Kim, J. Li, and T.-C. Tsao, "Two-Parameter Robust Repetitive Control with Application to a Novel Dual-Stage Actuator for Noncircular Machining," *IEEE/ASME Transactions on Mechatronics*, 2004, vol. 9, pp 644-652.
- [11] G. Pipeleers, B. Demeulenaere, J. De, Schutter, and J. Swevers, "Robust High-Order Repetitive Control: Optimal Performance Trade-Offs," *Automatica*, 2008, vol. 40, pp 2628-2634.
- [12] J.-H. She, M. Fang, Y. Ohyama, H. Hashimoto, and M. Wu, "Improving Disturbance-Rejection Performance Based on an Equivalent-Input-Disturbance Approach," *IEEE Transactions on Industrial Electronics*, 2008, vol. 55, pp 380-389.
- [13] J.-H. She, X. Xin, and Y. Pan, "Equivalent-Input-Disturbance Approach—Analysis and Application to Disturbance Rejection in Dual-Stage Feed Drive Control System," *IEEE/ASME Trans. Mechatronics*, 2011, vol. 16, no. 2, pp 330-340.
- [14] W. S. Levine, *The Control Handbook*, FL: CRC Press, Boca Raton, 1996.
- [15] K. Zhou and J. C. Doyle, *Essentials of Robust Control*, Prentice Hall, Upper Saddle River, New Jersey, 1998.
- [16] J. H. Moon, M. N. Lee, and M. J. Chung, "Repetitive Control for the Track-Following Servo System of an Optical Disk Drive," *IEEE Transactions on Control Systems Technology*, 1998, vol. 6, pp 663-670.
- [17] M. Steinbuch and M. L. Norg, "Advanced Motion Control: An Industrial Perspective," *European Journal of Control*, 1998, pp 278-293.